Osmotic Water Permeability of *Necturus* Gallbladder Epithelium

CALVIN U. COTTON, ALAN M. WEINSTEIN, and LUIS REUSS

From the Department of Physiology and Biophysics, The University of Texas Medical Branch, Galveston, Texas 77550; and Department of Physiology, Cornell University Medical College, New York, New York 10021

ABSTRACT An electrophysiological technique that is sensitive to small changes in cell water content and has good temporal resolution was used to determine the hydraulic permeability (L_p) of *Necturus* gallbladder epithelium. The epithelial cells were loaded with the impermeant cation tetramethylammonium (TMA^+) by transient exposure to the pore-forming ionophore nystatin in the presence of bathing solution TMA^+. Upon removal of the nystatin a small amount of TMA^+ is trapped within the cell. Changes in cell water content result in changes in intracellular TMA^+ activity which are measured with intracellular ion-sensitive microelectrodes. We describe a method that allows us to determine the time course for the increase or decrease in the concentration of osmotic solute at the membrane surface, which allows for continuous monitoring of the difference in osmolality across the apical membrane. We also describe a new method for the determination of transepithelial hydraulic permeability (L_p^t). Apical and basolateral membrane L_p's were assessed from the initial rates of change in cell water volume in response to anisosmotic mucosal or serosal bathing solutions, respectively. The corresponding values for apical and basolateral membrane L_p's were 0.66×10^{-3} and 0.38×10^{-3} cm/s·osmol/kg, respectively. This method underestimates the true L_p values because the nominal osmotic differences ($\Delta\Pi$) cannot be imposed instantaneously, and because it is not possible to measure the true initial rate of volume change. A model was developed that allows for the simultaneous determination of both apical and basal membrane L_p's from a unilateral exposure to an anisosmotic bathing solution (mucosal). The estimates of apical and basal L_p with this method were 1.16×10^{-3} and 0.84×10^{-3} cm/s·osmol/kg, respectively. The values of L_p for the apical and basal cell membranes are sufficiently large that only a small (<3 mosmol/kg) transepithelial difference in osmolality is required to drive the observed rate of spontaneous fluid absorption by the gallbladder. Furthermore, comparison of membrane and transepithelial L_p's suggests that a large fraction of the transepithelial water flow is across the cells rather than across the tight junctions.

Address reprint requests to Dr. Calvin U. Cotton, Department of Physiology and Biophysics, The University of Texas Medical Branch, Galveston, TX 77550.

J. GEN. PHYSIOL. © The Rockefeller University Press · 0022-1295/89/04/0649/31 $2.00
Volume 93 April 1989 649–679

INTRODUCTION

Several epithelia, including renal proximal tubule, intestine, and gallbladder, transport salt and water in near isosmotic proportions (Curran and Solomon, 1957; Diamond, 1962, 1978, 1979; Whitlock and Wheeler, 1964; Schafer et al., 1975, 1977, 1978; Andreoli et al., 1978; Bishop et al., 1979; Hill, 1980; Berry, 1983; Spring, 1983). In some tissues (e.g., *Necturus* gallbladder), a great deal is known about the routes, mechanisms, and properties of salt transport systems (Baerentsen et al., 1983; Reuss, 1983, 1984, 1989; Reuss and Costantin, 1984; Weinman and Reuss, 1984; Reuss and Stoddard, 1987); however, there is less information about the water transport pathway(s). Osmotic coupling of salt and water is a generally accepted mechanism of water transport in epithelia that absorb salt and water in isosmotic proportions. Demonstration of osmotic coupling requires the determination of the magnitude of the osmotic driving force and the hydraulic water permeability of the epithelial barriers. Progress in this area is hampered by the existence of unstirred layers adjacent to the cell membranes and by the complex geometry of epithelia, e.g., cellular and paracellular pathways (Pedley and Fischbarg, 1980; Barry and Diamond, 1984). Transepithelial measurements alone do not distinguish between cellular and paracellular pathways. In other words, it is necessary to use methods that examine the properties of individual components of the epithelium (i.e., apical membrane, basolateral membrane, tight junction, and lateral intercellular space).

Three groups of investigators have developed and applied techniques to measure membrane osmotic water permeability of *Necturus* gallbladder epithelium. Persson and Spring (1982) used an "optical sectioning" technique to measure changes in cell volume induced by exposure of the apical or basolateral cell membrane to anisosmotic solutions. Unfortunately, the time resolution of these studies was poor because a complete record of cell volume could be made at ~10-s intervals. A single "cross-sectional slice" was sampled more rapidly (0.6 s). However, it is uncertain whether such a method accurately resolves volume changes that result from changes in cell height or nonhomogenous changes in cell diameter (i.e., preferential changes in cell diameter at apical or basal pole, or cell membrane blebs). Although an effort was made in the studies of Persson and Spring (1982) to minimize unstirred layers (small, shallow chamber with rapid superfusion), the time required to establish the imposed difference in osmolality ($\Delta\Pi$) was not known. Zeuthen (1982) measured with microelectrodes the rate of change of intracellular Na^+, K^+, and Cl^- activities after exposure to an anisosmotic bathing solution. Although the time resolution was good, it was necessary to assume constancy of intracellular salt content. The calculated initial rate of cell volume changes was used to calculate membrane L_p's. Again, an effort was made to minimize unstirred layers and make rapid solution changes (small fluid compartment with rapid superfusion), but the time course for arrival or removal of the osmotic solute was unknown.

A similar approach was taken by Reuss (1985) and Cotton and Reuss (1986) except that tetramethylammonium (TMA^+) was introduced into the cells to serve as an impermeant intracellular volume marker. K^+-sensitive, liquid-membrane microelectrodes are known to be far more sensitive to quarternary ammonium ions than to K^+ (Neher and Lux, 1973); thus small amounts of intracellular TMA^+ can be

sensed. The major advantage of this technique is that practically no TMA^+ leaks out of the cells and changes in cell water can be monitored almost continually (usually at 100-ms intervals). A method was also described to determine the apparent unstirred layer thickness. Once the unstirred layer thickness is known, the time course for arrival or removal of the osmotic solute may in principle be calculated. Unfortunately, the relative contributions of the time required for the bulk solution mixing and for diffusion within the unstirred layer could not be determined, and hence it was not possible to accurately predict the time course for arrival of a solute at the membrane.

The experiments described in this article were designed to measure transepithelial, apical membrane, and basal membrane osmotic water permeabilities. We describe a new technique to measure transepithelial osmotic water permeability and the intracellular TMA^+ technique is used to measure changes in cell water volume in response to anisosmotic bathing solutions. Furthermore, we describe a method by which the time course for the generation of an imposed $\Delta\Pi$ can be monitored directly near the membrane. The data are fit to a model and the calculated L_p's are compared to estimates of L_p determined from linearization of initial rates without correction for unstirred layers. The results of these studies indicate that estimates of osmotic water permeability calculated from the "initial rate" of change in cell water volume upon exposure to an anisosmotic bathing solution are underestimates, in error by at least a factor of 2 in *Necturus* gallbladder epithelium. Our estimates of apical and basolateral L_p (1.2×10^{-3} and 0.8×10^{-3} cm/s·osmol, respectively) are sufficiently large that osmotically driven spontaneous fluid absorption would require a small transepithelial $\Delta\Pi$ (~3.3 mosmol/kg). Finally, our estimates of membrane L_p's and transepithelial L_p ($\sim 1 \times 10^{-3}$ cm/s·osmol/kg) are similar, and therefore transepithelial water flow may be largely via a cellular route.

METHODS

Tissue and Solutions

Necturus maculosus were maintained in aquaria at 5–10°C. The animals were anesthetized by immersion in a 1 g/liter solution of tricaine methanesulfonate. Gallbladders were removed, opened, rinsed free of bile, and mounted in a chamber, apical side up. For some experiments in which it was necessary to make rapid solution changes at the serosal surface, the tissue was mounted serosal side up, and small metal hooks were used to dissect away much of the subepithelial connective tissue. In the dissected preparation it was possible to make microelectrode impalements across the basolateral cell membrane. The upper compartment of the chamber was open, had a volume of ~0.1 ml, and was exchanged at a flow rate of 20–30 ml/min. The lower compartment was closed, had a volume of ~0.8 ml, and was perfused at a flow rate of 10–15 ml/min. A diagram of the chamber and electrode positions is presented in the preceding article (Cotton and Reuss, 1989).

The control bathing solution (NaCl Ringer's solution) contained 90 mM NaCl, 10 mM $NaHCO_3$, 2.5 mM KCl, 1.8 mM $CaCl_2$, 1.0 mM $MgCl_2$, 0.5 mM NaH_2PO_4 and was equilibrated with 1% CO_2/99% air. The pH was ~7.65 and the osmolality was ~200 mosmol/kg. During the TMA^+ loading procedure, the NaCl in the mucosal solution was replaced by TMA_2SO_4 (osmolality was maintained by addition of sucrose). After the cells were loaded with TMA^+ and the nystatin removed (see below), the epithelium was bathed on both sides with

isosmotic Ringer's solution in which 20 mM NaCl was omitted and osmolality was maintained by addition of sucrose (40 mM). Anisosmotic solutions were prepared by omission of 20 mM NaCl and varying the sucrose concentration (0, 20, 40, 60, 80, 100, and 120 mM). The changes in solution osmolality were nominally ±10, ±20, ±30, and ±40%. Actual osmolalities were measured with a vapor pressure osmometer (model 5100B; Wescor Inc., Logan, UT). In some experiments tetrabutylammonium chloride (TBACl) was added to the hyposmotic (1 mM), hyperosmotic (2 mM), and isosmotic (1 or 2 mM) solutions to serve as a marker for the arrival or disappearance of sucrose at the apical surface (see below).

Microelectrode Fabrication and Calibration

Glass microelectrodes were used to measure membrane voltages, intracellular TMA^+ activity, and extracellular TBA^+ activity. Cell membrane voltages and intracellular ion activities were determined by either simultaneous impalements of two cells with two single-barrel microelectrodes or by impalement with a double-barrel microelectrode. The single-barrel microelectrodes were prepared from borosilicate glass (1 mm o.d., 0.5 mm i.d.; Glass Company of America, Bargaintown, NJ) with internal fiber. Conventional microelectrodes were filled with 3 M KCl and had resistances that ranged from 20 to 50 MΩ when immersed in Ringer's solution. Single-barrel, TMA^+-sensitive microelectrodes were prepared by baking micropipettes overnight in an oven at 200°C. Hexamethyldisilazane (Sigma Chemical Co., St. Louis, MO) was introduced into the oven and the electrodes were baked for an additional 1–2 h. A short column of resin (potassium tetrakis [*p*-chlorophenylborate], 5 mg in 0.1 ml of 3-nitro-*O*-xylene) was introduced into the shaft and the tips were allowed to fill. The electrodes were back-filled with NaCl Ringer's solution and a chloridized silver wire was inserted and sealed in place with dental wax. The resistances ranged from 10 to 15 GΩ when immersed in NaCl Ringer's solution. Double-barrel microelectrodes were prepared from fused borosilicate glass (each barrel 1.0 mm o.d.; 0.5 mm i.d.; Hilgenberg, Malsfeld, Federal Republic of Germany). The fused doublet was heated, twisted 360°, allowed to cool down, and then pulled (PD-5 microelectrode puller, Narishige, Tokyo, Japan). The reference barrel was partially filled with deionized water and the other barrel was partially filled with hexamethyldisilazane. The electrodes were placed on a hot plate under a stream of hot air until the silane, and then the water, evaporated completely. The electrodes were heated under the same conditions for an additional 1–2 h. The reference barrel was filled with a 1 M Na formate/0.01 M KCl solution. A drop of liquid ion-exchange resin (potassium tetrakis [*p*-chlorophenylborate] or Corning Cl^- exchanger 477913, Corning Medical, Medfield, MA) was introduced into the silanized barrel. When necessary, bubbles were removed by gentle local heating with a microforge. The resin barrel was backfilled with NaCl Ringer's solution and a chloridized silver wire was sealed in each barrel for electrical connections. The resistance of the conventional barrel usually exceeded 400 MΩ and the resistance of the resin barrel was usually 100–200 GΩ. High-selectivity (TMA^+) microelectrodes were consistently obtained only after breaking the tips of the double-barrel electrodes by impaling the tissue. Useful electrodes had resistances of 80–150 MΩ (conventional barrel), 5–10 GΩ (TMA^+-selective barrel), and 30–60 GΩ (Cl^--selective barrel).

Single-barrel extracellular TBA^+-sensitive microelectrodes were prepared as described above except that prior to silanization the electrode was broken to a tip diameter of 1–3 μm. The electrode tip was filled with a cocktail that contained: potassium tetrakis (*p*-chlorophenylborate), 5 mg/0.1 ml in 3-nitro-*O*-xylene, 10% wt/vol polyvinyl chloride. Tetrahydrofuran (~20% vol/vol) was added to reduce the viscosity of the resin (Marban et al., 1980). The electrodes were prepared, and then allowed to cure for 24–48 h before use. Electrode resistance was <2 GΩ when immersed in Ringer's solution. Incorporation of polyvinyl chloride

into the microelectrode cocktail was necessary to polymerize the resin and prevent loss from the large tip of the microelectrode.

TMA^+-sensitive electrodes were calibrated with solutions that contained 120 mM KCl plus 0.1–20 mM TMACl. Slopes ranged from 54 to 62 mV/log [TMA^+] and the selectivity ratio for (TMA^+/K^+) was 10^2 to 10^3. The results of intracellular measurements were expressed as TMA^+ concentration, which assumes the activity coefficient inside and outside the cell is the same. TBA^+-sensitive electrodes were calibrated with solutions that contained NaCl Ringer's solution plus 0.1–10 mM TBA^+. Slopes were constant above 0.5 mM TBA^+ and ranged from 58 to 60 mV/log [TBA^+]. The selectivity ratios (TBA^+/K^+ and TBA^+/Na^+) measured with pure salt solutions (0.5, 1, and 2 mM) were $>10^6$. The Cl^--sensitive microelectrodes were calibrated with solutions that contained Hepes (1 mM)-buffered isotonic sucrose mixed with NaCl Ringer's solution (50% Ringer's or 10% Ringer's). Slopes were corrected for the difference in ionic strength and ranged from 52 to 58 mV/log [Cl^-].

Electrical Measurements

The transepithelial voltage (V_{ms}) was referred to the lower fluid compartment. The lower compartment electrode was a Ag-AgCl pellet in series with a Ringer's/agar bridge. The upper compartment electrode was a calomel half-cell in series with a flowing saturated KCl macroelectrode constructed from a fiber-filled glass pipette (Ultrawick; World Precision Instruments, New Haven, CT) pulled to a tip diameter of ~1 mm which was placed in the upper compartment, next to the suction (outflow) pipette. At the superfusion rates used, the KCl leakage into the mucosal solution compartment did not elicit measurable elevations in K^+ activity. Apical (V_{mc}) and basolateral (V_{cs}) membrane voltages were referred to the adjacent bathing solutions. Ion-sensitive microelectrodes were connected to a high input-impedance electrometer (model FD-223; World Precision Instruments). The Ag-AgCl pellet in the lower compartment served as ground. Extracellular microelectrodes were positioned and intracellular impalements were made with hydraulic micromanipulators (model MO-103, Narishige). The tissue was observed with a microscope (Diavert, E. Leitz, Inc., Rockleigh, NJ) equipped with Hoffman modulation-contrast optics at ×300.

Transepithelial constant current pulses (usually 50 $\mu A/cm^2$, 2–3-s duration) were passed between an Ag-AgCl pellet in the lower compartment and an Ag-AgCl wire in the upper compartment. The resulting voltage deflections were corrected for series solution resistance and used to calculate transepithelial resistance (R_t) and the apparent ratio of cell membrane resistances ($R_a/R_b = \Delta V_{mc}/\Delta V_{cs}$).

Membrane voltages (V_{ms}, V_{mc}, and V_{cs}) and differential ion-sensitive electrode voltages (V_{TMA^+}-V_{cs}, V_{Cl^-}-V_{cs}, and V_{TBA^+}-V_{ms}) were amplified, displayed on an oscilloscope (Tektronix, Inc., Beaverton, OR), digitized (instrument computer model 1074; Nicolet Instrument Corp., Madison, WI), and stored (Northstar Horizon Microcomputer, San Leandro, CA) for subsequent analysis. Each channel was usually sampled at 10 Hz.

Measurement of Transepithelial L_p

The transepithelial hydraulic permeability (L_p^t) was estimated from the initial rate of change of the concentration of TMA^+ (10 mM) in a thin layer of mucosal bathing solution upon stopping mucosal superfusion. In all cases, the mucosal solution was control Ringer's and the tissue had been exposed for at least 20 min to a serosal bathing medium of the same or different osmolality prepared as described above.

Both surfaces of the tissue were first superfused at a high rate (>30 ml/min). Then, the apical flow was stopped, and by suction through a small-tip, fire-polished pipette the mucosal solution was reduced (in 3–5 s) to a layer ~100 μm thick. To this end, the suction pipette was

mounted at a known angle and advanced with a calibrated, remote-control manipulator until it made contact with the cells. Then the pipette was withdrawn by a distance calculated to result in a height displacement of ~100 μm. The reproducibility of the height of the fluid layer after suction (<3%) was controlled by using a microelectrode to establish the position of the surface of the mucosal bathing solution as previously described (Reuss, 1984). The volume of the apical compartment at $t = 0$ was calculated from the height of the fluid layer and the cross-sectional area of exposed tissue.

A TMA^+-sensitive, double-barrel microelectrode was constructed as described above. Its tip was large (2–3 μm) and the reference barrel was filled with Ringer's solution to minimize leakage of electrolyte from the tip. The tip of this microelectrode was positioned 10–30 μm from the surface of the cells and the TMA^+ activity was measured as a function of time. J_v was calculated from the slope immediately after stopping superfusion, assuming conservation of TMA^+ and taking into account the height of the fluid layer. Inasmuch as such measurements were carried out with and without transepithelial osmotic gradients, the L_p^t was estimated from the difference between the J_v values (with gradient minus without gradient) and the difference in osmolality, assuming the sucrose reflection coefficient to be unity. This procedure corrected the J_v value for both spontaneous fluid transport and evaporation. The correction was always <20%.

TMA^+ Loading

The native membrane TMA^+ permeability is undetectably small, and therefore it was necessary to transiently increase the permeability in order to introduce TMA^+ into the intracellular compartment of the epithelium. The cells were loaded with TMA^+ as described previously (Reuss, 1985). Briefly, the tissue was mounted in the chamber and allowed to equilibrate for 60–90 min during bilateral perfusion with NaCl Ringer's solution. The mucosal compartment was then switched to TMA_2SO_4 Ringer's solution for ~2 min and then nystatin (10 mg/ml in dimethylsulfoxide) was added to the mucosal perfusate to a final concentration of 7.5–30 μg/ml (40–160 U/ml). After 5–10 min, the nystatin exposure was terminated and the mucosal TMA_2SO_4 Ringer's perfusion was continued until the membrane voltages and apparent ratio of cell membrane resistances recovered (usually 60–90 min) indicating "resealing" and restoration of the native membrane permselectivity. $SO_4^=$ was used in order to minimize the uptake of anions, since net uptake of salt and water during the loading procedure would result in cell swelling. A detailed validation of the reversibility of the exposure to nystatin, and the time course for restoration of the membrane properties has been presented previously (Reuss, 1985). Holz and Finkelstein (1970) showed that the effects of nystatin on water and ion permeability of lipid bilayers are linearly related. Therefore, the reversibility of the effect of nystatin on electrodiffusive ion permeation supports the notion that the water fluxes measured a long time after removal of the antibiotic are not mediated by nystatin remaining in the cell membranes.

Calculations

Intracellular TMA^+ concentration was calculated from V_{TMA^+}-V_{ca} for each data point. Changes in cell water volume were calculated from the following equation:

$$\Delta V(t) = [V(t) - V(0)] = V(0)\left[\frac{[TMA](0)}{[TMA](t)} - 1\right], \quad (1)$$

where $\Delta V(t)$ = cell water volume change (nl/cm^2), $V(t)$ = cell water volume at time = t (nl/cm^2), $V(0)$ = initial cell water volume (2,870 nl/cm^2), $[TMA^+](0)$ = intracellular $[TMA^+]$ at time = 0 (mM), $[TMA^+](t)$ = intracellular $[TMA^+]$ at time = t (mM). The value for initial cell

water volume was calculated for an epithelial sheet 35 μm tall with a cell water content of 82%. The initial rate of volume change is frequently used to calculate membrane L_p's. Our values will be compared with those obtained from a more elaborate model which is described below. The initial rate of change in cell water volume was calculated from a least squares linear regression of the first 10 s (see Fig. 1). Membrane hydraulic conductivity (L_p) was calculated from the following equation:

$$L_p = J_v/\sigma\,\Delta\Pi, \tag{2}$$

where L_p = hydraulic conductivity (cm/s·osmol), J_v = water flux (= ΔV, cm^3/cm^2·s), σ = osmotic solute reflection coefficient (assumed = 1 for sucrose), $\Delta\Pi$ = nominal imposed osmotic difference (osmol/kg). Since the initial-rate approximation and the use of the nominal $\Delta\Pi$ both lead to underestimates of L_p, we have also fit longer segments of the volume curve to a model that is described below.

To calculate the time course of the osmolality at the cell surface TBA^+ was used as a "sucrose tracer." A TBA^+-sensitive microelectrode was positioned near (1–3 μm) the cell surface, and the concentration of TBA^+ was calculated from V_{TBA^+} V_{ms} at each time point. The osmolality as a function of time was calculated from the following equation:

$$\Delta C_m(t) = \frac{[TBA^+]_m(t) - [TBA^+]_m(0)}{[TBA^+]_m(f) - [TBA^+]_m(0)}\,[C_b(f) - C_b(0)], \tag{3}$$

where $\Delta C_m(t)$ = change in osmolality of the mucosal solution adjacent to the apical membrane at time = t (mosmol/kg), $[TBA^+]_m(t)$ = concentration of TBA^+ at the apical cell membrane at time = t (mM), $[TBA^+]_m(0)$ = concentration of TBA^+ at the apical cell membrane before solution change (mM), $[TBA]_m(f)$ = steady-state concentration of TBA^+ at the apical cell membrane after solution change (mM), $C_b(f)$ = steady-state osmolality of bulk apical compartment after solution change, $C_b(0)$ = osmolality of bulk apical compartment before solution change.

Model Derivation

Changes in cell water volume in response to alterations in bathing solution osmolality were assessed using a model based on that developed by Weinstein and Stephenson (1981). The epithelium and adjacent layers consist of four compartments: mucosal solution (M), cell (I), lateral intercellular space (E), and serosal solution (S). These compartments are separated by five barriers: apical, basal, and lateral cell membranes (subscripts MI, IS, and IE, respectively) and junction and interspace basement membrane (subscripts ME and ES). As discussed below, the barriers whose properties can be assessed experimentally are "lumped equivalents" of tissue structures more complicated than the cell membrane alone.

The mathematical formulation is based on four simplifying assumptions: (*a*) the lateral space undergoes rapid osmotic equilibration compared with the cell, (*b*) during the time interval of the measurements changes in cell solute content are negligible, (*c*) fractional changes in cell volume are small, and (*d*) there are no concentration gradients within the cell and bulk solutions are well mixed.

The osmolality of the lateral intercellular space is described by

$$C_E = \gamma_M C_M + \gamma_S C_S + \gamma_I C_I + \gamma_N N, \tag{4}$$

where C denotes osmolality, the subscripts indicate the compartments, N is net solute transport (active or passive), and the coefficients γ quantify the contributions of fluxes between the lateral space and the larger compartments (the solute transport coefficient being γ_N).

These osmotic contributions behave as a weighted average:

$$\gamma_M + \gamma_S + \gamma_I = 1 \tag{5}$$

The applicability of Eqs. 4 and 5 to an epithelial model will be shown in the Appendix. There the coefficients γ will be given meaning in terms of individual membrane permeabilities. In brief, γ_S will be a measure of the interspace basement membrane salt permeability, γ_I will reflect the cell membrane water permeability, and γ_M will embody both solute and water permeabilities of the tight junction.

To consider the small changes in the system during an experimental maneuver it is convenient to represent the model variables as the sum of a steady-state value (when bathing media are equal) plus a small perturbation: $C_\alpha^0 + \Delta C_\alpha(t)$, osmolality of compartment α; $V^0 + \Delta V(t)$, cell water volume. If cell solute content changes little over the time course of interest

$$[C_I^0 + \Delta C_I(t)]\,[V^0 + \Delta V(t)] = C_I^0 V^0, \tag{6}$$

so that when fractional changes in osmolality and volume are small, $\Delta C_I(t)\Delta V(t) \sim 0$ and

$$\Delta V(t) = -\frac{V^0}{C_I^0}\Delta C_I(t). \tag{7}$$

The mass balance equation for cell volume is

$$\frac{d\Delta V}{dt} = J_{vMI} - J_{vIE} - J_{vIS}, \tag{8}$$

where

$$\begin{aligned} J_{vMI} &= L_{MI}(C_I - C_M) \\ J_{vIE} &= L_{IE}(C_E - C_I) \\ J_{vIS} &= L_{IS}(C_S - C_I). \end{aligned} \tag{9}$$

In Eqs. 8 and 9 $J_{v\beta}$ is the transmembrane volume flux, and L_β is the water permeability (RTL_p) of membrane β. Using the approximation for interspace osmolality, C_E, from Eq. 4 one obtains

$$\frac{d\Delta V}{dt} = -a_M C_M - a_S C_S + a_I C_I - a_N N, \tag{10}$$

where

$$\begin{aligned} a_M &= L_{MI} + \gamma_M L_{IE} \\ a_S &= L_{IS} + \gamma_S L_{IE} \\ a_I &= L_{MI} + L_{IS} + L_{IE} - \gamma_I L_{IE} \\ a_N &= \gamma_N L_{IE} \end{aligned}$$

It will be important to note that Eq. 5 implies

$$a_M + a_S = a_I. \tag{11}$$

Subtraction of the steady-state terms from the right side of Eq. 10, using Eq. 7 to eliminate ΔC_I yields the fundamental mass balance equation:

$$\frac{d\Delta V}{dt} + \left(a_I \frac{C_I^0}{V^0}\right)\Delta V = -a_M \Delta C_M - a_S \Delta C_S. \tag{12}$$

The terms of the right-hand side of Eq. 12 represent changes in mucosal or serosal bath osmolality from an initial steady state. It may be noted that even if one can do only a mucosal experiment (e.g., $\Delta C_s = 0$) one may still determine both permeability coefficients, a_M and a_S. The initial rate of volume uptake is

$$\left.\frac{d\Delta V}{dt}\right]_{t=0} = -a_M \Delta C_M, \tag{13}$$

while at steady state

$$\Delta V = -\frac{a_M}{a_I}\frac{V^0}{C_I^0}\Delta C_M = -\frac{a_M}{a_M + a_S}\frac{V^0}{C_I^0}\Delta C_M. \tag{14}$$

Alternatively, when one knows the mucosal osmolality near the cell surface as a continuous function of time, one may formally integrate Eq. 12 to obtain Eq. 15, which can be evaluated numerically:

$$\Delta V(t) = -a_M \int_0^t \exp\left[a_I \frac{C_I^0}{V^0}(s - t)\right]\Delta C_M(s)ds. \tag{15}$$

Comparison of the values of ΔV predicted from Eq. 15 with those found experimentally permits the determination of the parameters a_M and a_I as the best fit of a least-squares procedure.

RESULTS

Estimates of Apical Membrane L_p from Initial Rate of Change in Cell Water Volume

The initial rate of change in cell water volume calculated from the change in intracellular TMA^+ concentration upon exposure to an anisosmotic mucosal bathing solution (±20%) was determined in nine tissues. An example of the change in cell water volume in response to a hyperosmotic mucosal solution ($\Delta\Pi$ = 0.035 osmol/kg) is illustrated in Fig. 1 *A*. An expanded segment, with the corresponding linear regression, is shown in Fig. 1 *B*. Upon return to isosmotic mucosal solution the cell water volume returned to the control value. The brief period of exposure to the anisosmotic bathing solutions used in these experiments resulted in small (<5 mV), slowly developing changes in membrane voltages. The initial rate of cell shrinkage for all tissues studied was 22.3 ± 1.9 nl/cm^2·s (0.78 ± 0.07%/s) and the initial rate of cell swelling was 25.7 ± 2.1 nl/cm^2·s (0.90 ± 0.07%/s) for hyperosmotic and hyposmotic mucosal solutions, respectively. The apparent apical membrane hydraulic conductivity can be calculated from the induced water flow and the nominal $\Delta\Pi$ according to Eq. 2. If we assume a reflection coefficient equal to one ($\sigma = 1$) for sucrose, the L_p is 0.62(±0.06) × 10^{-3} or 0.60(±0.05) × 10^{-3} cm/s·osmol/kg for hyperosmotic or hyposmotic mucosal solutions, respectively.

Water flow across a membrane will generally cause changes in electrolyte and nonelectrolyte concentrations in the unstirred fluid layers adjacent to the membrane (Barry and Diamond, 1984). For instance, osmotic water flow will cause dilution ("sweeping away") of solute adjacent to the membrane on the side into which water flows, and an increase in the concentration of solute at the membrane surface on the opposite side. The net effect is a reduction of the nominal transmembrane

(and transepithelial) osmotic gradients. This will give rise to apparent rectification of water permeability unless the true $\Delta\Pi$ is determined and used for the calculation of L_p. Furthermore, the geometry and/or dimensions of the lateral space may be altered by osmotic water flow, thereby causing rectification of water flow (Wright et al., 1972). Larger osmotic water flows will cause more severe problems; therefore, it is necessary to measure water flow in response to a range of osmotic differences. In a series of four experiments, the J_v was calculated from the initial rate (10-s linearization) of changes in cell water volume in response to several differences in osmolality ($\Delta\Pi$ = ±10%, ±20%, +30%, +40%). The results for both hyposmotic and hyperosmotic mucosal solutions are presented in Fig. 2 *A*. Over the range of osmolalities studied, J_v was linearly related to the nominal difference in osmolality with an L_p of 0.66×10^{-3} cm/s·osmol/kg. The constancy of the value of L_p is further illustrated in Fig. 2 *B*, in which L_p is plotted as a function of $\Delta\Pi$. These results are consistent with a nonrectifying water transport pathway. In contrast, Persson and Spring (1982) observed that the magnitude of J_v was independent of the imposed osmotic gradient, i.e., in the ranges of $\Delta\Pi$s of +5 to +20% and −5 to −20% the values of J_v were virtually constant.

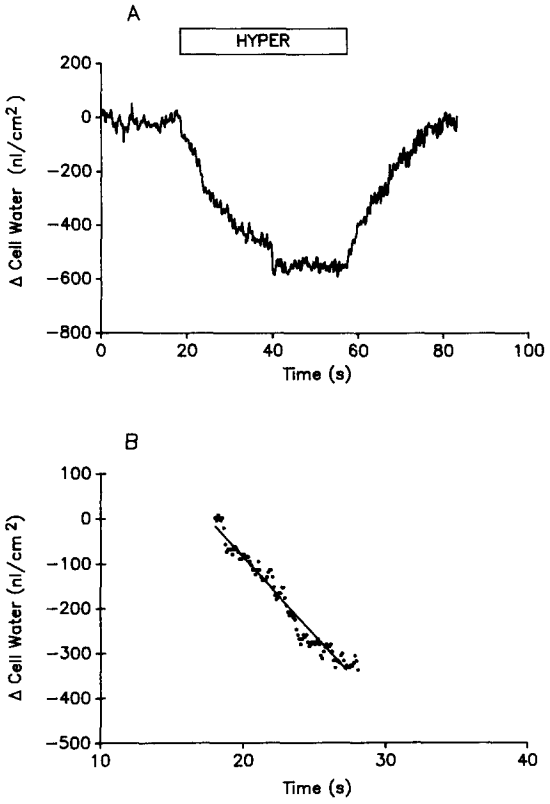

FIGURE 1. Change in cell water volume in response to a hyperosmotic mucosal bathing solution. (*A*) Mucosal solution osmolality was increased from 203 to 238 mosmol/kg water for ~40 s and then returned to control osmolality. The serosal solution osmolality remained constant (203 mosmol/kg water) throughout the experiment. In this and subsequent figures changes in cell water volume were calculated from the changes in intracellular TMA^+ concentration as described in Methods. The initial cell water volume was assumed to be 2,870 nl/cm² epithelium. (*B*) An expanded 12-s segment of the same experiment. The dashed line represents the least-squares linear fit during the first 10 s after the onset of the change in cell water volume. The correlation coefficient and the slope of the line are 0.98 and −35.0 nl/cm²·s, respectively.

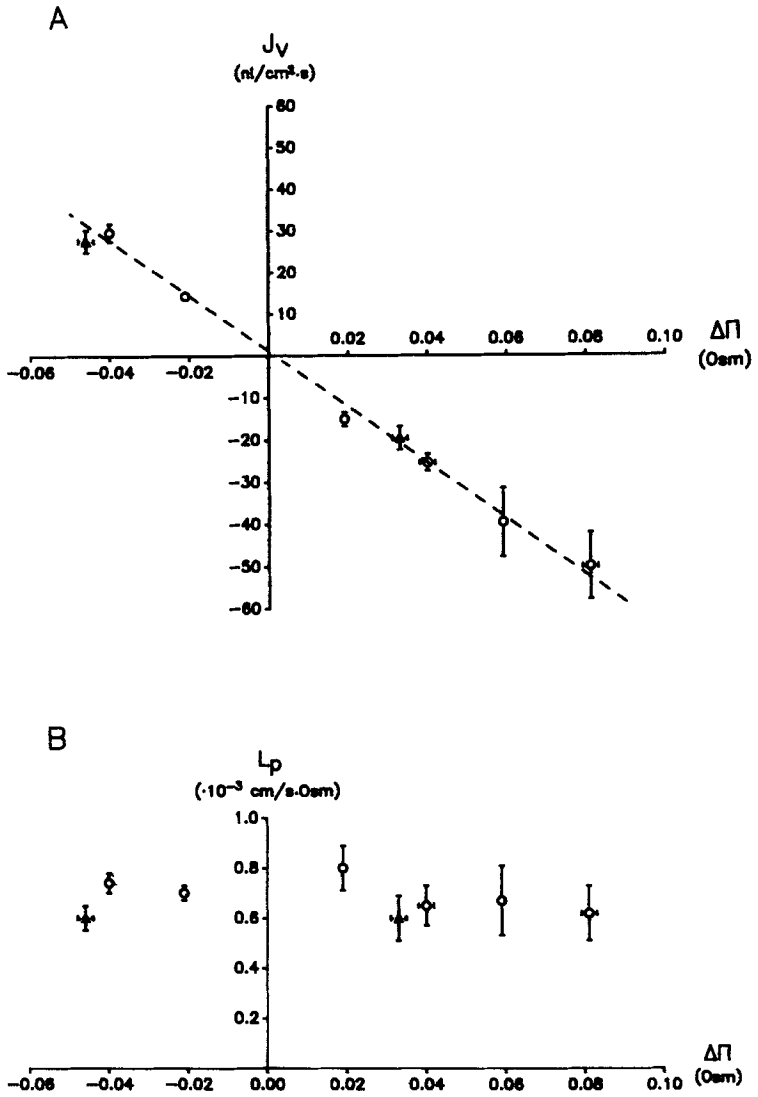

FIGURE 2. (*A*) The relationship between ΔΠ (apical) and J_v (apical). Four tissues (○) were exposed to a range of apical ΔΠ's and the resulting J_v was calculated from the initial rate (10-s least squares linear regression) of change in cell water volume. Five additional tissues (▲) were exposed to ~±20% change in mucosal solution osmolality. Vertical and horizontal bars represent the standard errors for J_v and ΔΠ, respectively. Two tissues were used for ΔΠ = ±10%. The dashed line is the weighted (by the number of tissues at each point) least-squares regression for the four tissues studied at several ΔΠ's. $J_v = 1.21–661\ \Delta\Pi$; $r^2 = 0.90$. The slope of the line is the hydraulic water permeability, $L_p = 0.66 \times 10^{-3}$ cm/s·osmol/kg. (*B*) The L_p is calculated for each point shown in *A*. Over the range of ΔΠ's studied L_p is constant.

Estimates of Basolateral Membrane L_p from Initial Rates of Change in Cell Water Volume

Similar experiments were done to assess the basolateral membrane L_p. Although much of the subepithelial connective tissue was removed by dissection (see Methods), it was not possible to make impalements with double-barrel, TMA^+-sensitive microelectrodes through the remaining layers of connective tissue. This is due to the larger tip diameter of the double-barrel, TMA^+-sensitive microelectrodes (see Methods). Consequently, we used intracellular Cl^- as our cell volume marker for the basolateral studies (for the problems associated with the use of Cl^- as a volume

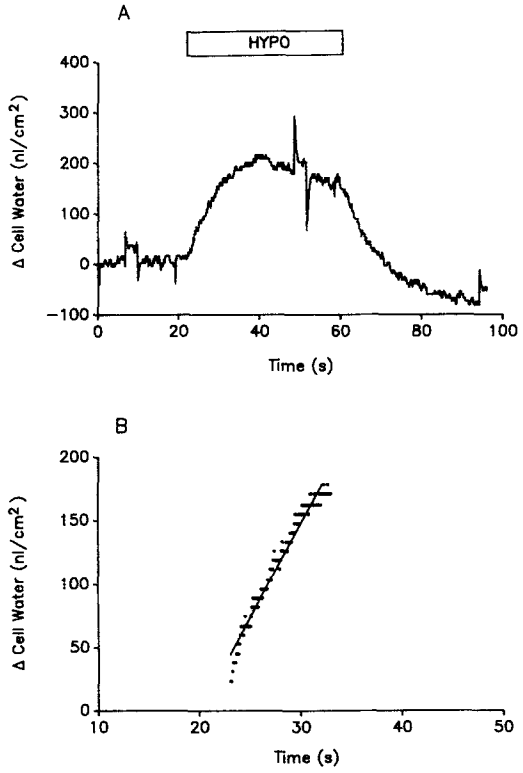

FIGURE 3. Change in cell water volume in response to a hyposmotic mucosal bathing solution. (*A*) Serosal solution osmolality was decreased from 195 to 156 mosmol/kg water for ~40 s and then returned to control osmolality. The serosal solution osmolality remained constant (195 mosmol/kg water) throughout the experiment. The initial cell water volume was assumed to be 2,870 nl/cm² epithelium. (*B*) Expanded 12-s segment of the same record. The dashed line represents the least-squares linear fit during the first 10 s after the cell water volume began to change. The correlation coefficient and the slope of the line are 0.98 and 14.6 nl/cm²·s, respectively.

marker, see Discussion). The initial rate of change in cell water volume, calculated from the change in intracellular Cl^- activity in response to anisosmotic serosal bathing solutions, was determined in eight tissues. An example of the cell volume change in response to a hyperosmotic serosal solution ($\Delta\Pi$ = 0.039 osmol/kg) is illustrated in Fig. 3 *A*. An expanded segment with the corresponding linear regression is shown in Fig. 3 *B*. The initial rate of cell shrinkage was 16.1 ± 2.5 nl/cm²·s (n = 8) and the initial rate of cell swelling was 15.6 ± 2.4 nl/cm²·s (n = 8) for hyperosmotic (~20%) and hyposmotic (~20%) serosal solutions, respectively. The corresponding basolateral membrane L_p's were 0.42(±0.07) × 10^{-3} cm/s·osmol/kg (hyperosmotic) and 0.43(±0.06) × 10^{-3} cm/s·osmol/kg (hyposmotic).

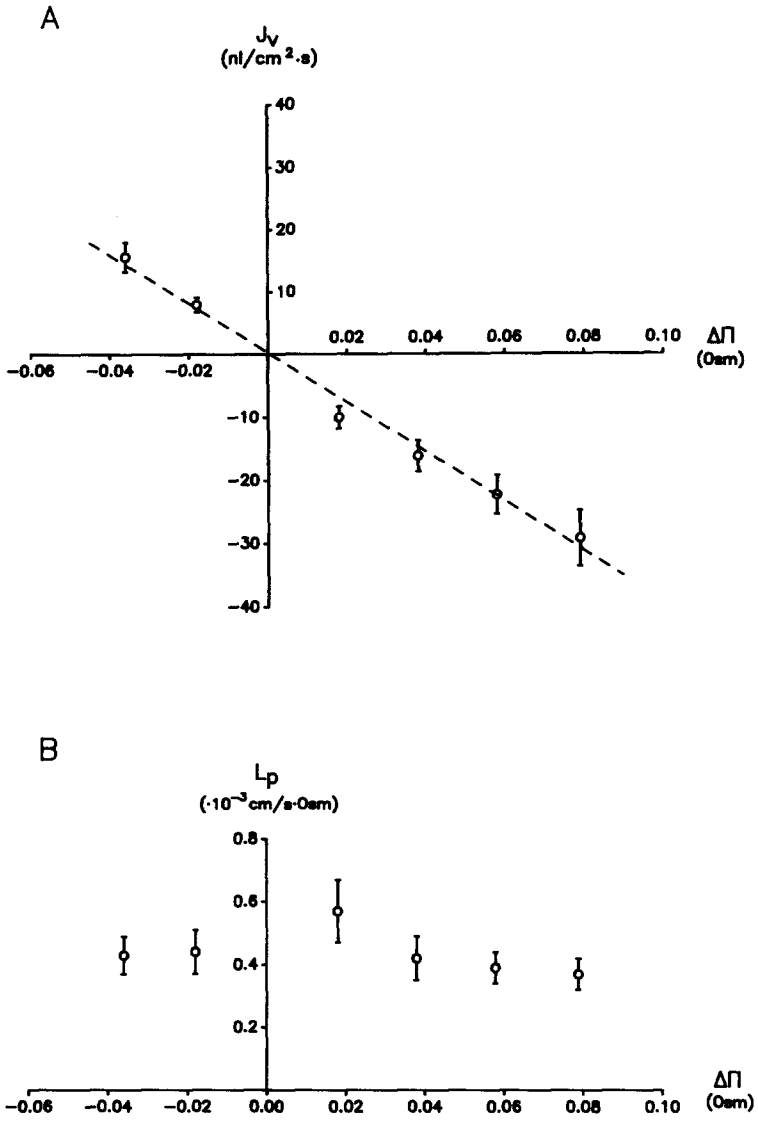

FIGURE 4. (*A*) The relationship between ΔΠ (basolateral) and J_v (basolateral). Eight tissues were exposed to a range of serosal ΔΠ's and the resulting J_v was calculated from the initial rate (10-s least squares linear regression) of change in cell water volume. Four tissues were used for +10%, six tissues for −10%, and eight tissues at all other osmolalities. Vertical and horizontal bars represent the standard errors for J_v and ΔΠ, respectively. The dashed line is the weighted (by the number of tissues at each point) least squares linear regression. J_v = 0.27–391 ΔΠ; r^2 = 0.82. The slope of the line is the hydraulic water permeability, L_p = 0.39 × 10^{-3} cm/s·osmol/kg. (*B*) The L_p is calculated for each point shown in *A*. Over the range of ΔΠ's studied L_p is constant.

Tissues were exposed sequentially to several different anisosmotic serosal bathing solutions ($\Delta\Pi$ = ±10%, ±20%, +30%, and +40%) and the initial rate of change of cell water was used to calculate L_p. The results are presented in Fig. 4 *A*. Over the range of osmolalities studied J_v was linearly related to the nominal $\Delta\Pi$ with an L_p of 0.38×10^{-3} cm/s·osmol/kg. The constant value of basolateral L_p is further illus-

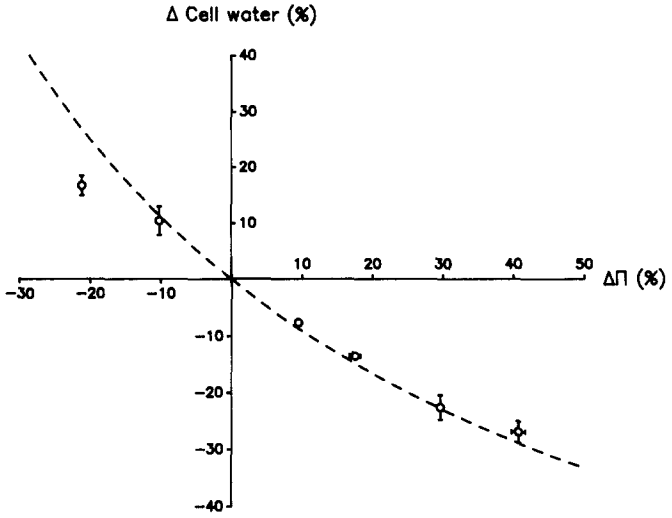

FIGURE 5. Steady-state changes cell water volume in response to anisosmotic mucosal bathing solutions. The cells were assumed to be at osmotic equilibrium (200 mosmol/kg water) prior to exposure to anisosmotic mucosal solutions. Two tissues were used for ±10%, nine tissues for ±20%, and four tissues for +30% and +40%, respectively. Vertical and horizontal bars represent standard errors for L_p and $\Delta\Pi$, respectively. The dashed line is the predicted relationship between $\Delta\Pi$ and Δ cell water volume, assuming: (*a*) an initial cell water volume of 2,870 nl/cm^2, (*b*) initial intracellular and extracellular osmolality of 200 mosmol/kg water, (*c*) no net loss or gain of intracellular solute during the interval of exposure to the anisosmotic solution, and (*d*) no water flow across the basal membrane into the bulk serosal solution compartment. The theoretical line was calculated from the equation

$$\frac{V(f) - V(0)}{V(0)} \times 100 = \left[\frac{C_m(0)}{C_m(f)} - 1\right] \times 100,$$

where $V(0)$ = initial cell water volume, $V(f)$ = cell water volume at steady state, $C_m(0)$ = initial mucosal solution osmolality, $C_m(f)$ = nominal mucosal solution osmolality after solution change.

trated in Fig. 4 *B* in which L_p is plotted as a function of $\Delta\Pi$. The results are similar to those elicited by exposure to anisosmotic mucosal solutions (see above).

Steady-State Changes in Cell Water Volume

The "steady-state" changes in cell water volume in response to mucosal anisosmotic solutions are illustrated in Fig. 5. With the exception of the value for 20% hyposmotic solutions the data points fall on the dashed line describing ideal osmometric behavior, i.e., depicting a cell in osmotic equilibrium across the apical membrane,

with no net gain or loss of intracellular solute, and with no water flux across the basal membrane. This result suggests that water flow across the basal membrane is small and that osmotic equilibration between the cell and the bulk serosal solution does not occur during exposure to anisosmotic mucosal solutions, which is compatible with: (*a*) low basal membrane water permeability, (*b*) small basal membrane surface area, and/or (*c*) the existence of a small subepithelial compartment in series with the cell, which prevents equilibration with the bulk serosal solution (Curran

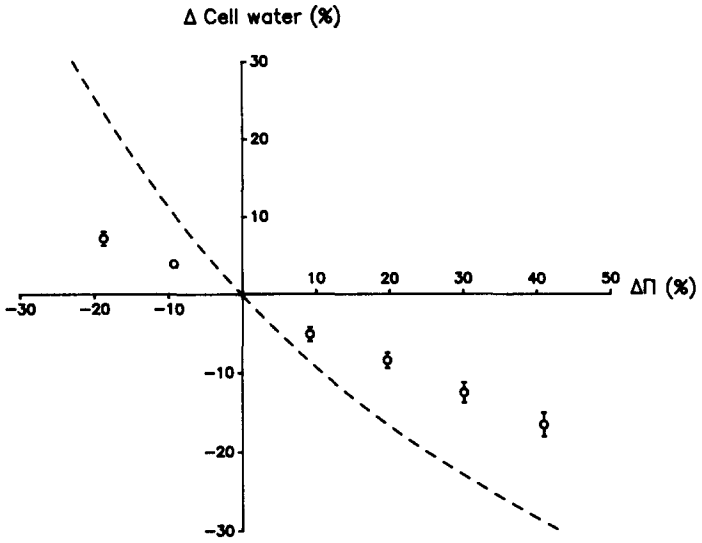

FIGURE 6. Steady-state changes of cell water volume in response to anisosmotic serosal bathing solutions. The cells were assumed to be at osmotic equilibrium (200 mosmol/kg water) prior to exposure to anisosmotic serosal solutions. Four tissues were used for +10%, six for −10%, and eight at all other osmolalities. Vertical and horizontal bars represent standard errors for L_p and ΔΠ, respectively. The dashed line is the predicted relationship between ΔΠ and the change in cell water volume assuming: (*a*) an initial cell water volume of 2,870 nl/cm^2, (*b*) initial intracellular and extracellular osmolality of 200 mosmol/kg water, (*c*) no net loss or gain of intracellular solute, and (*d*) no water flow across the apical membrane into the bulk mucosal solution compartment. The line was calculated from the equation

$$\frac{V(f) - V(0)}{V(0)} \times 100 = \left[\frac{C_s(0)}{C_s(f)} - 1\right] \times 100,$$

where, $V(0)$ = initial cell water volume, $V(f)$ = cell water volume at steady state, $C_s(0)$ = initial serosal solution osmolality, $C_s(f)$ = nominal serosal solution osmolality after solution change.

and MacIntosh, 1962). Each of these conditions could contribute to prevent osmotic equilibration between the cell and the bulk serosal bathing solution.

The corresponding steady-state changes in cell water volume in response to serosal anisosmotic solutions are illustrated in Fig. 6. The dashed line is the calculated change in cell water volume for a cell that behaves as a perfect osmometer across the basolateral membrane. With both hyperosmotic and hyposmotic serosal bathing

solutions the observed change in cell water volume is significantly less than that predicted for an osmometric response. Such a relationship suggests that there may be appreciable water flow across the apical membrane, net flux of Cl^-, or both, in response to anisosmotic serosal bathing solutions.

Simultaneous Determination of Apical and Basal L_p's

Experiments were done in seven tissues in which the apical membrane was exposed to anisosmotic bathing solutions that contained TBA^+ in order to monitor simulta-

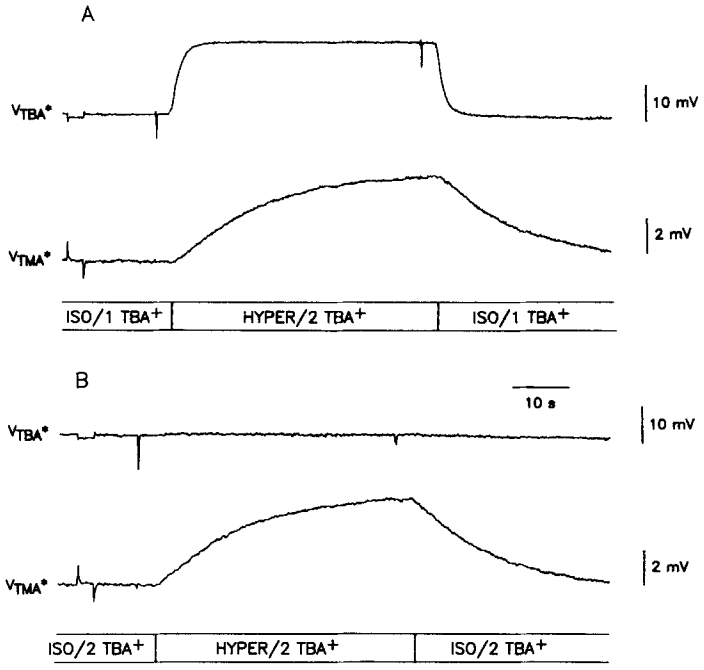

FIGURE 7. Changes in mucosal solution osmolality and cell water volume upon exposure to a hyperosmotic mucosal bathing solution. (*A*) The upper trace is the output of a TBA^+-sensitive extracellular microelectrode placed near the apical membrane and referred to the serosal solution ($V_{TBA^*} = V_{TBA} - V_{ms}$), and the lower trace is the output of a TMA^+-sensitive microelectrode inside the cell, referred to the basolateral membrane voltage ($V_{TMA^*} = V_{TMA} - V_{cs}$). During the indicated interval the solution was changed from an isosmotic solution containing 1 mM TBACl to an hyperosmotic solution containing 2 mM TBACl. The downward spikes in the V_{TBA^*} trace are due to activation of a solenoid valve to change the bathing solution. The 3-s pulse near the beginning of each trace is the response to a small transepithelial current pulse. The downward deflection in the V_{TBA^*} trace is due to the mucosal solution resistance (i.e., the TBA^+ electrode is adjacent to the apical membrane, whereas the reference macroelectrode is positioned 3–5 mm above the surface of the epithelium). The spikes in the V_{TMA^*} trace represent the different response times of the conventional voltage-sensing and the ion-sensing microelectrode barrels. (*B*) A similar solution change is made ~5 min later. In this case, the $[TBA^+]$ was the same in the isosmotic and the hyperosmotic solutions. Note that the two cell volume traces are essentially identical.

neously the rate of osmotic solute arrival to or removal from the apical surface, and the resulting change in cell water content. An example of the voltage traces from such an experiment is presented in Fig. 7. Since the intracellular TMA^+ electrode is also sensitive to TBA^+, it was necessary to demonstrate that over the period of exposure to elevated [TBA^+] there is no detectable entry of TBA^+ into the cellular compartment. Fig. 7 shows two voltage traces depicting changes in cell water volume in which the [TBA^+] was either raised (*A*) or maintained constant (*B*) during the expo-

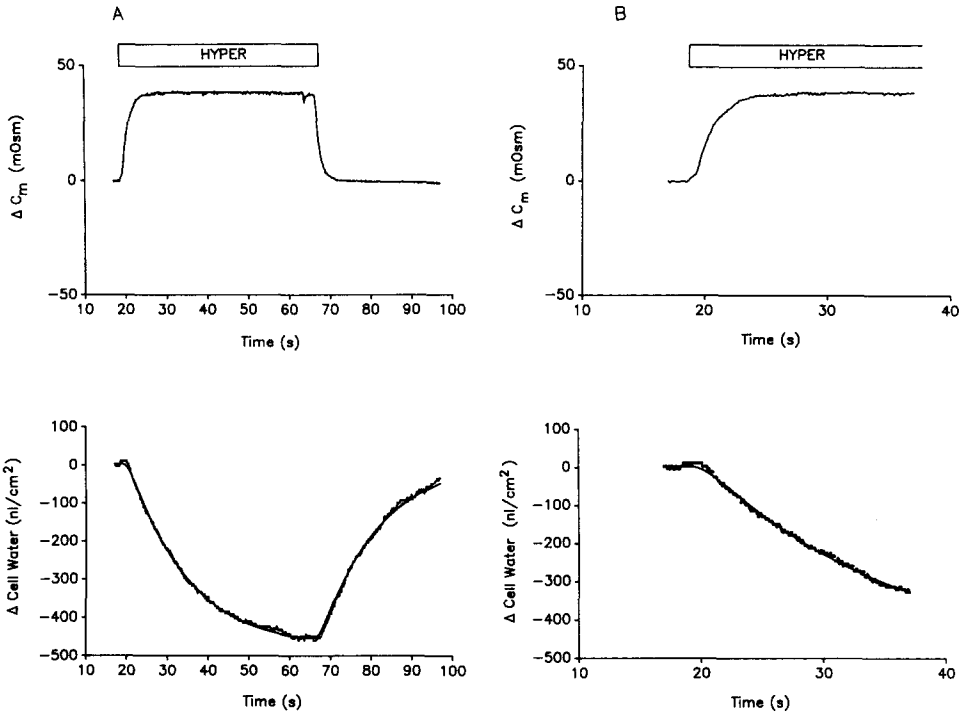

FIGURE 8. Changes in mucosal solution osmolality, cell water volume, and the fitted change in cell water volume in response to exposure to a hyperosmotic mucosal solution. (*A*) The mucosal solution osmolality was increased from 206 to 244 mosmol/kg water. The initial cell water volume was assumed to be 2,870 nl/cm^2. The data for the complete experiment (~70 s) are fit to the model described in Methods. The estimates of apical and basal L_p's are 0.87×10^{-3} and 0.09×10^{-3} cm/s · osmol/kg, respectively. (*B*) Same experiment as above except that the fit spans only 20 s. The estimates of apical and basal L_p's are 0.90×10^{-3} and 0.10×10^{-3} cm/s · osmol/kg, respectively.

sure to hyperosmotic bathing solutions, as evident in the upper trace in each panel. The voltage traces in Fig. 7, *A* and *B*, are not different; therefore the changes in mucosal solution [TBA^+] do not affect the intracellular TMA^+ signal.

Fig. 8 illustrates the time course for an increase in osmolality at the apical cell membrane (*A*, upper trace) and the resultant changes in cell water volume (*A*, lower trace) in response to an increase in mucosal solution osmolality. In the lower trace

of each panel the smooth solid line is the "fitted" curve for the data. The results of a similar experiment in which the mucosal solution was made hyposmotic are illustrated in Fig. 9. In most studies, tissues were exposed to anisosmotic mucosal bathing solutions for 40 s. Individual traces were fit (as described in Methods) over a short interval, chosen to include most of the change in cell water volume (20 s) and over a longer interval (60 s) that included essentially the whole period of exposure to the anisosmotic solution. The fitted and calculated parameters are listed in Table 1 for both hyperosmotic and hyposmotic solutions at 20 and 60 s. Since the values

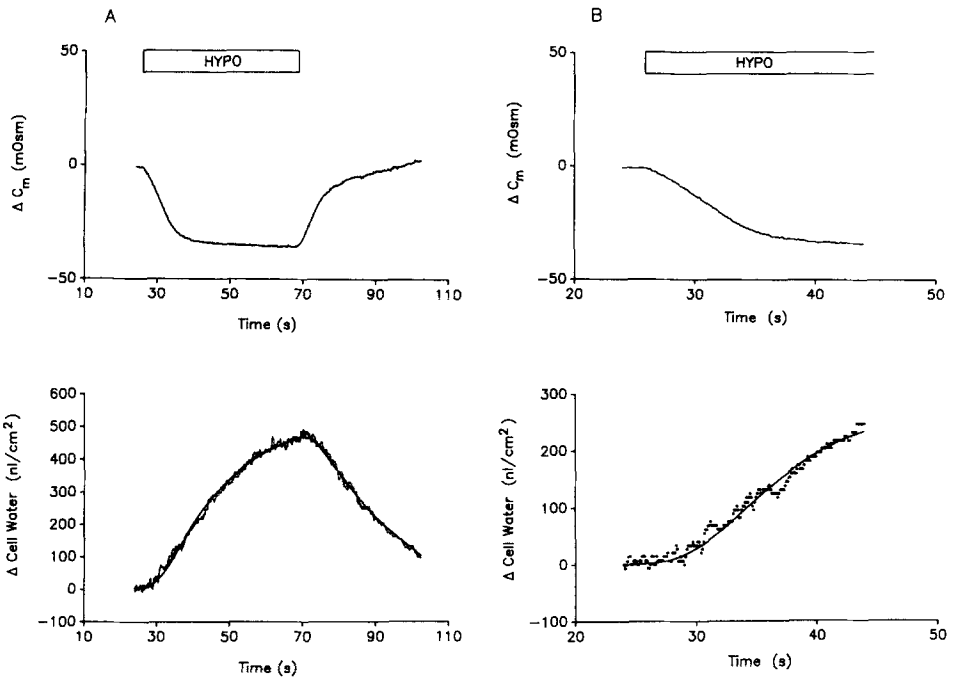

FIGURE 9. An example of the change in mucosal solution osmolality, cell water volume, and the fitted change in volume in response to exposure to a hyposmotic mucosal solution. (*A*) The mucosal solution osmolality was decreased from 206 to 163 mosmol/kg water. The initial cell water volume was assumed to be 2,870 nl/cm^2. The data for the complete experiment (~70 s) are fit to the model described in Methods. The estimates of apical and basal L_p's are 0.72×10^{-3} and 0.08×10^{-3} cm/s · osmol/kg, respectively. (*B*) Same experiment as above except that only 20 s of data are fit to the model. The estimates of apical and basal L_p's are 0.69×10^{-3} and 0.17×10^{-3} cm/s · osmol/kg, respectively.

in hyperosmotic and hyposmotic solutions were not significantly different, the pooled data are also presented. The only significant difference between 20-s and 60-s fits was in the estimation of a_s.

Transepithelial Hydraulic Permeability

The transepithelial hydraulic permeability (L_p^t) was measured, as described in Methods. Typical records of the changes in [TMA^+] are shown in Fig. 10. The J_v values

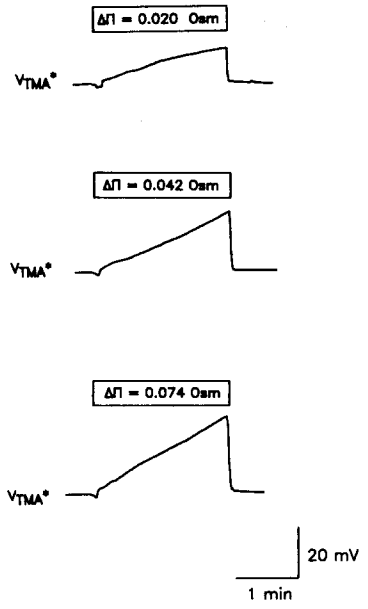

FIGURE 10. Transepithelial water flow. The mucosal surface was superfused with an isosmotic bathing solution that contained 10 mM TMA^+. The serosal surface was exposed to a solution that was hyperosmotic by 20, 42, or 72 mosmol/kg. Mucosal superfusion was halted and all but a thin (~100 μm) layer of solution was rapidly removed. The change in V_{TMA^*} ($=V_{TMA} - V_{ms}$) indicates net flux of water from the mucosal to the serosal bath. After 2 min, mucosal superfusion was resumed and V_{TMA^*} returned to baseline.

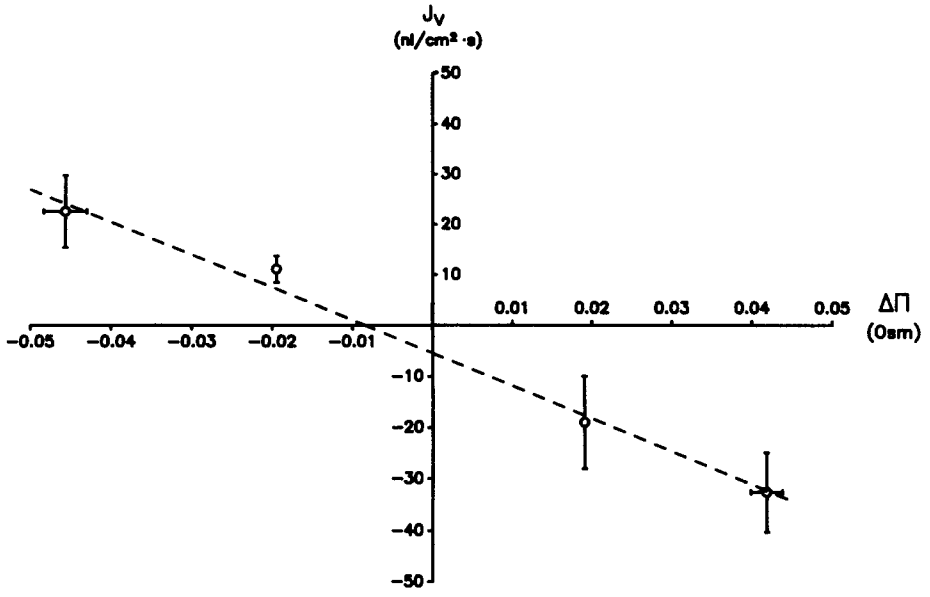

FIGURE 11. The relationship between J_v and transepithelial ΔΠ. The initial rate of change of mucosal solution [TMA^+] after interrupting mucosal superfusion was used to calculate J_v (see Methods). Positive values of J_v represent net serosa-to-mucosa water movement (i.e., hyposmotic serosal solution), whereas negative values of J_v represent net mucosa-to-serosa water movement (i.e., hyperosmotic serosal solution). Two tissues were used for ΔΠ = −0.020, four for ΔΠ = +0.020, six for ΔΠ = −0.045, and 10 for ΔΠ = +0.042 osmol/kg. The vertical and horizontal bars represent standard errors of J_v and ΔΠ, respectively. The dashed line represents the weighted least squares linear regression. $J_v = -5.47–642\ \Delta\Pi$; $r^2 = 0.64$. The slope of the line is the hydraulic water permeability, $L_p^t = 0.64 \times 10^{-3}$ cm/s·osmol/kg.

obtained in 22 measurements in 10 tissues are plotted in Fig. 11, as functions of the difference in osmolality. The L_p^i values ranged from 0.14 to 1.87 $\times$ 10^{-3} cm/s·osmol/kg, with a mean of 0.64 $\times$ 10^{-3}. The variability of the results was largely due to differences from tissue to tissue and not among determinations in each individual preparation.

DISCUSSION

Several models and theoretical treatments have been formulated to account for isosmotic fluid absorption in tubular and planar epithelia (Curran and MacIntosh, 1962; Diamond and Bossert, 1967; Hill, 1975a, b, 1980; Sackin and Boulpaep, 1975; Schafer et al., 1975; Schafer et al., 1977; Hill and Hill, 1978; Diamond, 1979; Weinstein and Stephenson, 1981). Unfortunately, the assumptions and predictions have proved difficult to validate and demonstrate experimentally (see Diamond, 1979; Hill, 1980; Reuss and Cotton, 1988). For example, in all models, the osmolality of the transported fluid depends critically on the cell membrane water permeability, but as Diamond and others have pointed out (see Barry and Diamond, 1984), unstirred fluid layers adjacent to or located within the epithelium certainly cause underestimates of transepithelial and transmembrane water permeability, at least in planar epithelia.

In this article, we illustrate the application of new techniques to study transepithelial water transport. These techniques include the use of intracellular microelectrodes to estimate changes in cell water volume and the use of extracellular electrodes to determine the rate of arrival or departure of an osmotic solute at the apical membrane surface and thereby assess the true osmotic gradient as a function of time. The major advantages of these techniques are their sensitivity and temporal resolution. The cell water and extracellular osmolality data allow us to calculate the apparent water permeabilities of both the apical and basal membranes from exposure to an anisosmotic mucosal bathing solution.

Calculation of Apical Membrane L_p from Initial Rates of Change of Cell Water Volume

Although exposure of the apical cell membrane to anisosmotic mucosal bathing solutions produced changes in cell water volume that were reasonably linear over the first 5–10 s (see Fig. 1), we will show that this observation alone does not justify calculation of L_p's from apparent initial rates. In the simplest possible system, i.e., J_v is a linear function of L_p and $\Delta\Pi$ (Eq. 2), the rate of change in cell water volume upon an instantaneous change in bath osmolality is not constant with time due to the change in cell osmolality elicited by water flow. For this reason L_p will be underestimated. Furthermore, the delivery of osmotic solute to the membrane depends upon convective mixing in the bulk solution and diffusion through the unstirred fluid layer. Thus, an instantaneous, step change in solution osmolality cannot be achieved (Diamond, 1979), which results in a further underestimate of L_p. Other events are likely to occur that would reduce J_v, i.e., osmotic gradient dissipation due to solvent drag and water flow across the opposite membrane. For these reasons, the apparent linearity of J_v in experiments in which the problems above are probable, is in all likelihood fortuitous. In general, the greater the L_p, the more significant

these errors become (Barry and Diamond, 1984). Therefore, the estimates of L_p from the initial rate of volume change and the nominal $\Delta\Pi$ are certainly underestimates.

We found a linear relationship between $\Delta\Pi$ and J_v (i.e., constant L_p) over the range of osmotic differences used in this study (−20% to +40%). In contrast, Persson and Spring (1982) found that J_v remained virtually constant for $\Delta\Pi$'s between −18% and +18%. These authors suggested that the anomalous behavior was the result of unstirred layer phenomena, presumably via solute polarization within the unstirred layer, i.e., dilution of solute adjacent to the membrane in the compartment into which water flows and increase in concentration of solute adjacent to the membrane in the opposite compartment. It is also possible that the time interval (three to five measurements at a rate of one measurement per 10 s) used by Persson and Spring to calculate the initial rate of change in cell volume was too long and may have influenced their estimates. If there is a systematic error introduced in the determination of initial rates for either small or large $\Delta\Pi$'s then the extrapolation to the L_p at zero $\Delta\Pi$ is not valid. Our value for apical membrane L_p calculated from initial rates and nominal $\Delta\Pi$'s was 0.66×10^{-3} cm/s·osmol/kg, i.e., close to that recalculated from the data of Zeuthen (1982) ($\sim 0.50 \times 10^{-3}$ cm/s·osmol/kg for a cell 35 μm tall with an intracellular water content of 82%) and with Persson and Spring (1982) (1.0×10^{-3} cm/s·osmol/kg from extrapolation to zero $\Delta\Pi$).

Thus far we have assumed that changes in cell water elicited by exposure to anisosmotic mucosal solutions result from water flow across the apical membrane exclusively. This may not be valid since the apical membrane and the tight junction are in parallel and water could cross the junctional complex and enter or exit the cell across the lateral (basolateral) membrane. The water permeability of the tight junction is unknown, but since the junctional area is only a small fraction of the apical surface area in *Necturus* gallbladder (<1%) a large junctional L_p would be necessary to accommodate the observed J_v. To the extent that the apical membrane L_p exceeds that of the basolateral membrane, water flow across the junction and basolateral membrane results in a smaller fractional error in the estimate of the apical membrane L_p. Without knowledge of the magnitude of the junctional L_p, we cannot accurately evaluate the contribution of this route to our estimates of "apical membrane L_p."

Calculation of Basolateral Membrane L_p from Initial Rates

Since we were unable to make impalements across the serosal connective tissue with double-barrel TMA^+ microelectrodes, we chose to use intracellular Cl^- as a marker for cell water volume. This approach is less desirable because Cl^- is not impermeant. Hence, underestimates could result from net Cl^- fluxes via either the native transport pathways or pathways activated or altered by cell volume changes. However, the changes in cell water volume were determined over a short interval and Cl^- fluxes caused by the changes in intracellular concentrations per se are probably small, based upon the net Cl^- transport rates across the cell membranes (Reuss, 1984).

We observed a linear relationship between J_v and $\Delta\Pi$ (i.e., constant L_p) across the basolateral membrane. The calculated L_p (0.38×10^{-3} cm/s·osmol/kg) was less than

that of the apical membrane. Zeuthen (1982) reported a basolateral L_p of 1.1×10^{-3} cm/s·osmol/kg, whereas the value reported by Persson and Spring (1982), of 2.2×10^{-3} cm/s·osmol/kg, was obtained by extrapolation to zero $\Delta\Pi$ from measurements with solutions that were 8.9% and 17% hyperosmotic. (J_v was 21.6×10^{-6} cm/s for the smaller $\Delta\Pi$ [8.9%] and 9.1×10^{-6} cm/s for the larger $\Delta\Pi$ [17%].) We have no explanation for the inverse relationship between J_v and $\Delta\Pi$ observed by Persson and Spring.

Steady-State Changes in Cell Water Volume

We found that exposure to hyperosmotic mucosal bathing solutions caused cell shrinkage, and at steady state the changes in cell water volume were not significantly different from those predicted for an osmometric response. Similarly, exposure to a 10% hyposmotic mucosal solution elicited an osmometric response. These results suggest that water flow across the opposite membrane (basolateral) is small, or that there exists a subepithelial compartment which is not in osmotic equilibrium with the serosal bath. In contrast, the steady-state swelling induced with a 20% hyposmotic mucosal solution was significantly less than expected. It has been suggested that hyperosmotic mucosal solutions "close" and hyposmotic mucosal solutions "open" the lateral intracellular spaces in gallbladder epithelium (Smulders et al., 1972; Wright et al., 1972; Reuss and Finn, 1977). Narrowing or widening of the lateral intracellular spaces would result in a decrease or an increase in diffusive exchange between the lateral space and the bulk serosal fluid, respectively. Such responses would be consistent with the approach to and deviation from osmometric volume changes with hyperosmotic and hyposmotic mucosal bathing solutions, respectively. The results of the experiments in which apical and basal membrane L_p's were determined from a mucosal solution change indicate that there is water flow across both membranes and an osmometric response would not be expected. However, at 30–40 s the changes in cell water volume were nearly osmometric (Fig. 5). This observation is not in contradiction with the conclusion of a finite basal membrane L_p, since the latter reflects primarily the water flow over a short interval (~20 s). As longer time intervals are used to calculate membrane L_p's, the values of apical and especially basal L_p fall (see Table I).

In contrast, the steady-state volume changes in response to anisosmotic serosal bathing solutions were significantly less than predicted for osmometric behavior. This is not surprising for several reasons. First, while net flux of Cl^- during early times is likely to be small, this may not hold for longer intervals (i.e., 30 s after the osmotic perturbation). Secondly, our results suggest that apical membrane L_p is approximately twice the value of the basal membrane; since at the steady state the volume change is a weighted average of the apical and basal L_p's (Eq. 4), the volume change should be significantly less than predicted for osmotic equilibration across the basolateral membrane only. In accord with the argument presented above for the effects of "opening" and "closing" the lateral spaces, we would predict that hyposmotic serosal solutions would close the lateral spaces, thereby allowing the cell to approach osmotic equilibrium across the apical rather than the basal cell membrane. The larger fractional deviation with 20% hyposmotic than with 20%, 30%, or 40% hyperosmotic serosal solutions is consistent with this interpretation. Although

it is tempting to draw conclusions from these arguments, caution must be exercised, especially in experiments in which Cl^- serves as the intracellular volume marker since we have no information about the contribution of net transmembrane Cl^- fluxes under these conditions.

Our results are not in agreement with those of Persson and Spring (1982), in which osmometric responses were observed with either mucosal or serosal anisosmotic bathing solutions. We do not understand how osmometric responses can be obtained at both the apical and the basolateral membranes during unilateral anisosmotic substitutions, unless there is always a small compartment on the side of the epithelium opposite to the side on which the solution change is made, and such a compartment prevents appreciable mixing with the bulk solution. These authors describe a predicted linear relationship between the magnitude of $\Delta\Pi$ and the change in cell volume (Fig. 7, Persson and Spring, 1982). From the relationship between $\Delta\Pi$ and the change in cell water volume (Figs. 5 and 6), it is clear that the predicted relationship is not linear. If expressed as a change in cell volume, rather than cell water volume, the relationship would still not be linear. Since Persson and Spring (1982) pooled the data for mucosal and serosal anisosmotic solutions, it is not possible for us to determine whether or not the cells truly showed osmometric responses.

Simultaneous Determination of Apical and Basal L_p's

As discussed above there are several shortcomings inherent in the calculation of membrane L_p from the "initial rate" of change in cell volume, including (*a*) uncertainty about the time course for establishing the osmotic gradient, (*b*) inaccuracies inherent in measurements of small changes in cell volume, since they must be made over short intervals, and (*c*) the need to experimentally evaluate apical and basolateral cell membranes individually. The method we have developed and the model we have used to analyze the data circumvent each of these problems. The osmolarity at the apical membrane surface is determined experimentally, the entire cell volume transient or a portion thereof can be analyzed, and estimates of apical and basal L_p are obtained from a single unilateral osmotic perturbation.

In some respects, the model chosen has no direct anatomic correlates. The "apical" and "basal" barriers to water flow are not only the corresponding cell membranes, but also include the adjacent unstirred fluid layers, both anatomic (intracellular and subepithelial tissue compartments) and hydrodynamic (serosal fluid compartment). Since these complications increase the resistance to osmotic water flow, the true cell membrane L_p's are higher than the parameters estimated for the model. As explained in Table I, the permeabilities calculated from the model fit (a_M, a_S, a_I) are lumped permeabilities. For instance, a_M has the dimensions of L_p (i.e., a hydraulic permeability coefficient), but in principle, includes the L_p of the apical membrane (without correction for folding) and of the junctions; if junctional L_p were zero, $a_M = L_p$ (apical). The basal parameter a_S includes the basal region of the basolateral cell membrane and the series elements between cell and bulk serosal solution. The model assumption of rapid osmotic equilibration of the lateral space with the cell removes the lateral cell membrane from the estimate of basolateral L_p.

The apparent L_p values determined from initial rates of change in cell water volume are also lumped parameters, that include parallel and/or series elements, as described above. Therefore, the coefficients obtained with this technique can be compared to those resulting from model fits. Since we cannot instantaneously impose a step change in osmolality at the membrane and since there may be some water flow across the opposite membrane we expect the L_p calculated from the initial rate of change in cell water volume to represent an underestimate of the true membrane water permeability. It is therefore of interest to compare directly the estimate of L_p calculated from initial rates with the estimate of apical membrane L_p determined from the 20-s fit to the model. The ratio of "initial rate L_p" to "model fit L_p" for 18 traces in eight tissues was 0.49 ± 0.05. Since the values are similar (i.e., they differ only by a factor of 2) and since the discrepancy is in the predicted direction, the two approaches support one another. A direct comparison cannot be made in the same tissues between estimates of basolateral membrane L_p from the

TABLE I

Membrane Hydraulic Conductivity

Parameter	20-s fits			60-s fits		
	Hyposmotic	Hyperosmotic	Pooled	Hyposmotic	Hyperosmotic	Pooled
	10^{-3} cm/s · osmol/kg					
a_M	1.13	1.18	1.16	0.85	0.98	0.92
	(±0.23)	(±0.14)	(±0.12)	(±0.06)	(±0.13)	(±0.08)
a_S	1.07	0.66	0.84	0.38	0.21	0.29
	(±0.45)	(±0.23)	(±0.23)	(±0.14)	(±0.10)	(±0.09)
a_I	2.17	1.83	1.98	1.22	1.19	1.20
	(±0.68)	(±0.34)	(±0.34)	(±0.20)	(±0.21)	(±0.14)
n	5	6	7	5	6	7

The values are means ± SEM. The meaning of the fitted parameters is outlined in Methods (see model derivation): a_M, a_S, and a_I have units of hydraulic conductivity (L_p) and the values of a_M and a_S may be compared directly with the estimates of apical and basolateral membrane L_p obtained from the initial rates of volume change according to Eq. 2. The anisosmotic mucosal solutions were ~±0.04 osmol/kg and the period of exposure was ~40 s; n is the number of tissues.

two approaches, but the averages obtained from separate groups also differ by about twofold (model fit $L_p = 0.84(\pm 0.23) \times 10^{-3}$ cm/s·osmol/kg, initial rate $L_p = 0.38 \times 10^{-3}$ cm/s·osmol/kg). This result is not surprising since on average 5–7 s was required for the osmotic solute (sucrose) to attain 95% of the steady-state concentration at the membrane. Therefore, the time-averaged $\Delta\Pi$ would be significantly less than the nominal $\Delta\Pi$ used for the calculation of L_p from the initial rate of change in cell water volume. The magnitude of the error introduced by noninstantaneous imposition of the nominal osmotic gradient and by the inability to measure true initial rates will increase as the osmotic water permeability increases.

Four simplifying assumptions were necessary for the formulation of the model. First, changes in cell water volume are small. In each of the experiments the $\Delta\Pi$ was ±20% which resulted in ~15% changes in cell water volume. Secondly, during the measurement, changes in cell solute content are negligible. Although we have no direct evidence to support this assumption, the observation that upon return to isos-

motic mucosal bathing solution the cell water volume returned to control values suggests that there was little net solute flux. In contrast, Fisher et al. (1981) reported a peak volume change followed by rapid return to the control volume, and then a transient overshoot in the opposite direction upon the return to isosmotic bathing solutions. We have never observed such a response during the 30–50-s exposure to anisosmotic bathing solutions. It is possible that volume regulation processes are not significantly activated during these short exposures to anisosmotic solutions. Furthermore, water permeability (diffusive or osmotic) is several orders of magnitude greater than the resting permeability of the gallbladder to Na^+, K^+, or Cl^-. Thirdly, we assumed rapid osmotic equilibration between the lateral intercellular space and the cell. We have no data that bear direcly on this issue, but morphometric studies reveal that the lateral spaces are long, narrow, convoluted slits with a large surface-to-volume ratio. If the value of the lateral cell membrane L_p is similar to our estimates of apical or basal membrane L_p, then the large surface area and small volume of the lateral space would likely allow for rapid osmotic equilibration with the cell.

Finally, the additional problem of solute polarization within the unstirred fluid layers (mucosal, serosal, and intracellular compartments) must be examined. In the presence of unstirred layers, water flux across a barrier causes changes in solute concentration at the membrane-solution interface. The magnitude of the polarization depends upon unstirred layer thickness (δ), linear velocity of water flow (v), and the diffusion coefficient of the solute (D_s). The relationship can be described by the following equation (House, 1974):

$$\frac{C_m}{C_b} = \exp\left[\pm \frac{v\delta}{D_s}\right] \tag{16}$$

where C_m = concentration of solute at the cell surface, C_b = concentration of solute in the bulk solution, "+" and "−" refer to accumulation and depletion of solute in the *cis* and *trans* sides of the membrane, respectively, defined by the water flows. We previously reported mucosal solution unstirred layers between 70 and 120 μm (Cotton and Reuss, 1985; Reuss, 1985). These values are overestimates, since the extent to which mixing in the bulk solution influenced our measurement of unstirred layer thickness was underestimated. More recent experiments, in which the time required for bulk solution mixing is distinguished from that for diffusion through the unstirred layer, suggest that the effective thickness of the unstirred layer is only 25–40 μm. (See the preceding article in this issue.) If we assume a mucosal unstirred layer of δ = 50 μm, a solute diffusion coefficient of 10^{-5} cm^2/s, and a linear velocity for water flow of 0.3×10^{-4} cm/s, we calculate from Eq. 16 that the osmolality of the solution adjacent to the apical cell membrane is 99.5% or 100.5% of the bulk solution osmolality (240 or 160 mosmol/kg water for hyperosmotic and hyposmotic mucosal solutions, respectively). In contrast, the unstirred layer on the basal side is at least 200 μm (anatomic unstirred layer due to subepithelial connective tissue). With similar values of v and D_s, the osmolality at the basal membrane would differ by ±6% from the bulk solution osmolality (200 mosmol/kg water). In combination, the transepithelial $\Delta\Pi$ would be reduced from the nominal value of 40 mosmol/kg to 25 mosmol/kg. The effect is greater if any or all of the water flow is funneled

through a portion of the surface area, i.e., through the lateral intercellular spaces and/or the tight junctions. The most serious consequence of this effect is probably the estimate of basolateral L_p from the model, since it assumes no polarization of solute at the basolateral (or apical) cell membrane. Thus, if polarization does occur $\Delta\Pi$ basal is reduced and L_p basal will be underestimated. The impact of solute polarization upon the calculations of initial rate is difficult to evaluate quantitatively; the direction of the effect is to underestimate the cell membrane L_p's.

Two technical problems in the determination of $\Delta\Pi$ must be addressed. The TBA^+-sensitive microelectrode is located a few micrometers from the apical membrane, and therefore a small error is introduced since the solute is required to diffuse the additional 3–5 μm between the electrode and the cell surface. Inasmuch as diffusion over such short distances is rapid, the error (an overestimate of $\Delta\Pi$) is likely to result in only a small underestimate in L_p. Secondly, the diffusion coefficient for TBA^+ (0.76×10^{-5} cm^2/s) is somewhat greater than that for sucrose (0.52×10^{-5} cm^2/s). Consequently, the establishment of $\Delta\Pi$ calculated from the change in [TBA^+] will be an overestimate and again will result in a small underestimate of L_p. The magnitude of these errors will increase as the thickness of the unstirred layer increases, but the errors are likely to be small under our experimental conditions.

Transepithelial L_p

Many of the problems in the measurement of cell membrane L_p's also arise in the measurement of transepithelial L_p^t. We estimated a value of L_p^t of 0.64×10^{-3} cm/s·osmol/kg. If we assume that water flow across the tight junction is zero, then we can calculate the hydraulic conductivity of the cellular path (L_p^c) from our estimates of a_M and a_S (conductances in series). L_p^c calculated from the 20-s model fits (Table I) is 0.49×10^{-3} cm/s·osmol/kg and agrees reasonably well with the value of L_p^t. Inasmuch as the apical and basal L_p's estimated from both 60-s fits and initial rates were lower, the agreement is not as good. In addition, the transepithelial L_p is likely an underestimate, since the experiments were done by generating a steady-state $\Delta\Pi$ across the tissue; consequently, there is a net flux of water across the tissue and thus solute polarization is at a maximum in the serosal compartment. Since the mucosal perfusion is stopped for the measurement there will be an unstirred layer of ~100 μm on the mucosal side. If we assume an apical unstirred layer of 100 μm and a serosal unstirred layer of 200 μm, we can estimate the extent to which L_p^t would be underestimated based upon the observed J_v. The error, dependent upon the direction of water flow, is about a factor of 2.

Osmotic Gradient and Route of Water Flow during Spontaneous Fluid Absorption

Since the goal of these studies is to understand isosmotic fluid transport, it is instructive to determine the total transepithelial osmotic gradient necessary to drive the observed rate of fluid absorption by *Necturus* gallbladder epithelium. For a spontaneous rate of fluid absorption of 12 μl/cm^2·h (Davis and Finn, 1985; Reuss, 1984) and a transepithelial L_p of ~1×10^{-3} cm/s·osmol/kg, a $\Delta\Pi$ of only 3.3 mosmol/kg water would be sufficient. The osmotic difference ($\Delta\Pi$) will include luminal hypotonicity and serosal hypertonicity. Osmotic differences of this magnitude are

not easily measured. It is therefore not surprising that no transepithelial osmotic gradients have been detected during spontaneous fluid absorption in gallbladder epithelium (Diamond, 1964; Ikonomov et al., 1985).

Similarity of individual membrane and transepithelial L_p's does not prove that fluid transport is via a cellular route, although it suggests that the transcellular L_p is of sufficient magnitude to allow for transepithelial fluid absorption with a small osmotic gradient. As we discussed above, it is likely that both membrane and transepithelial L_p's are underestimates. The variability in both sets of determinations (see Table I and Fig. 11) does not allow for a firm conclusion of a significant difference between them. In fact, although the similarity of membrane and transepithelial L_p values suggests a cellular route for fluid absorption, a different experimental approach will be required to establish this with certainty.

In summary, we have measured changes in cell water volume in response to anisosmotic bathing solutions with a technique that allows for measurements of small changes with good temporal resolution. We have also described a method to quantify the time course of the imposed osmotic gradient. Finally, we present a model that enables us to calculate the osmotic water permeability of the apical and basal barriers from a unilateral change in bathing solution osmolality. The results, together with estimates from the initial rates of volume change induced by anisosmotic bathing solutions, support the conclusion that the L_p's of the cell membranes of *Necturus* gallblader epithelium are very high. Transepithelial water transport could be by osmotic water flow predominantly or exclusively via the transcellular pathway.

APPENDIX

To justify the use of Eqs. 4 and 5 a nonelectrolyte model of the lateral interspace will be examined. The model is similar to that of Weinstein and Stephenson (1981), with difference that cell osmolality may be distinct from that of the luminal bath. Also represented is the possibility of electrically driven solute transport across tight junction and basement membrane.

Membrane subscripts, β

- ME Tight junction
- IE Lateral cell membrane
- ES Interspace basement membrane

Permeabilities

- L_β Water permeability
- σ_β Reflection coefficient
- h_β Solute permeability

Fluxes

- $J_{v\beta}$ Volume flux
- $J_{s\beta}$ Solute flux
- N_β Active (or electrically driven) solute transport

Compartments, α

- M Mucosal
- I Intracellular
- E Interspace
- S Serosal

Intensive variables

P_α Pressure

C_α Osmolality

Flux Eqs. A1–A3 describe mass transfer across tight junction, lateral cell membrane, and interspace basement membrane, respectively:

$$J_{vME} = -L_{ME}P_E + RTL_{ME}\sigma_{ME}(C_E - C_M),$$

$$J_{sME} = J_{vME}(1 - \sigma_{ME})C_o + h_{ME}(C_M - C_E) + N_{ME}; \tag{A1}$$

$$J_{vIE} = -L_{IE}P_E + RTL_{IE}\sigma_{IE}(C_E - C_I),$$

$$J_{sIE} = J_{vIE}(1 - \sigma_{IE})C_o + h_{IE}(C_I - C_E) + N_{IE}; \tag{A2}$$

$$J_{vES} = L_{ES}P_E,$$

$$J_{sES} = J_{vES}C_o + h_{ES}(C_E - C_S) + N_{ES}. \tag{A3}$$

These equations are linear due to an "isotonic convection approximation" in the description of solute flux, namely, replacement of the mean membrane concentration by a constant, reference concentration, C_o. It is also assumed that $\sigma_{ES} = 0$. The two equations for steady-state mass balance are

$$\begin{aligned} J_{vME} + J_{vIE} - J_{vES} &= 0; \\ J_{sME} + J_{sIE} - J_{sES} &= 0. \end{aligned} \tag{A4}$$

These are two linear equations in the two unknowns, C_E and P_E, the interspace osmolality and pressure.

The solution of these equations is tedious but straightforward. As in previous efforts, it helps to first define the permeability properties of an equivalent "mucosal" membrane, composed of tight junction and cell in parallel:

$$L_M = L_{ME} + L_{IE},$$

$$\sigma_M = (\sigma_{ME}L_{ME} + \sigma_{IE}L_{IE})/L_M,$$

$$h_M = h_{ME} + h_{IE} + RTC_0 \frac{L_{ME}L_{IE}}{L_M}(\sigma_{IE} - \sigma_{ME})^2,$$

and then, for ease of notation, some composite parameters:

$$L_M = \frac{L_M L_{ES}}{L_M + L_{ES}},$$

$$D = h_M + h_{ES} + RTL_{MS}C_0\sigma_M^2,$$

$$\tilde{D} = h_{IE} + RTC_0 \frac{L_{IE}}{L_M}\sigma_{IE}[L_{ME}(\sigma_{IE} - \sigma_{ME}) + L_{MS}\sigma_M],$$

$$N = N_{ME} + N_{IE} - N_{ES}.$$

It is found that

$$C_E = \left(\frac{D - \tilde{D} - h_{ES}}{D}\right)C_M + \frac{h_{ES}}{D}C_S + \frac{\tilde{D}}{D}C_I + \frac{N}{D}. \tag{A5}$$

Eq. A5 for C_E is of the form of Eq 4, where the coefficients satisfy Eq. 5. Eq. A5 may also be

rewritten as

$$C_E = \left(\frac{D - \tilde{D} - h_{ES}}{D}\right) C_M + \frac{h_{ES}}{D} C_S + \frac{\tilde{D}}{D} C_I + \frac{h_{ES}}{D} \hat{C},$$

where $\hat{C}$ is the "strength of transport" of the epithelium, i.e., the magnitude of the osmotic gradient required to nullify reabsorptive water flux (Weinstein and Stephenson, 1981). Now Eq. 4 has the particularly simple form for interspace osmolality as a weighted average

$$C_E = \gamma_M C_M + \gamma_S(C_S + \hat{C}) + \gamma_I C_I \ .$$

Considerable simplification is achieved when it is assumed that the cell membrane is relatively tight to solute:

$$h_{IE} = 0 \qquad \sigma_{IE} = 1.0$$

and that there is relatively little resistance to water flow out of the interspace:

$$L_{MS} \approx L_M \ .$$

In this case:

$$D \approx h_{ES} + h_{ME} + RTC_0(L_{ME}\sigma_{ME}^2 + L_{IE});$$
$$\tilde{D} \approx RTC_0 L_{IE}$$

so that the permeability coefficients of Eq. 10 may be written:

$$a_M = RT\left[L_{MI} + L_{IE}\left(\frac{h_{ME} + RTC_0 L_{ME}\sigma_{ME}^2}{D}\right)\right];$$
$$a_S = RT\left[L_{IS} + L_{IE}\left(\frac{h_{ES}}{D}\right)\right]. \qquad \text{(A6)}$$

Now it is easy to see the effect of a permeable tight junction to augment a_M above RTL_{MI}. One can also see that the contribution of the lateral cell membrane to a_S will be less than RTL_{IE}, since $h_{ES}/D < 1$. What this means is that any attempt to deliver solute immediately to the lateral cell surface will be limited by the finite solute permeability of the interspace basement membrane (i.e., an intraepithelial unstirred layer). This limitation figures prominently for either restricted solute movement (small h_{ES}) or rapid washout of the interspace (large L_{IE}).

We thank J. S. Stoddard and Y. Segal for their comments on a previous version of this manuscript. We also thank A. L. Pearce and Olwen H. Hooks for secretarial assistance.

This research was supported by National Institutes of Health grant DK-38588.

Original version received 16 May 1988 and accepted version received 8 September 1988.

REFERENCES

Andreoli, T. E., J. A. Schafer, and S. L. Troutman. 1978. Perfusion rate-dependence of transepithelial osmosis in isolated proximal convoluted tubules: estimation of the hydraulic conductance. *Kidney International.* 14:263–269.

Baerentsen, H., F. Giraldez, and T. Zeuthen. 1983. Influx mechanisms for Na^+ and Cl^- across the brush border membrane of leaky epithelia: a model and microelectrode study. *Journal of Membrane Biology.* 75:205–218.

Barry, P. H., and J. M. Diamond. 1984. Effects of unstirred layers on membrane phenomena. *Physiological Reviews.* 64:763–873.

Berry, C. A. 1983. Water permeability and pathways in the proximal tubule. *American Journal of Physiology.* 245:F279–F294.

Bishop, J. H. V., R. Green, and S. Thomas. 1979. Free-flow reabsorption of glucose, sodium, osmoles and water in rat proximal convoluted tubule. *Journal of Physiology.* 228:331–351.

Cotton, C. U., and L. Reuss. 1985. Measurement of the effective thickness of the mucosal unstirred layer in *Necturus* gallbladder epithelium. *Journal of General Physiology.* 86:44*a*. (Abstr.)

Cotton, C. U., and L. Reuss. 1986. Measurement of hydraulic water permeability (L_p) of the apical membrane of *Necturus* gallbladder epithelium. *Federation Proceedings.* 45:891. (Abstr.)

Curran, P. F., and J. R. MacIntosh. 1962. A model system for biological water transport. *Nature.* 193:347–348.

Curran, P. F., and A. K. Solomon. 1957. Ion and water fluxes in the ileum of rats. *Journal of General Physiology.* 41:143–168.

Davis, C. W., and A. L. Finn. 1985. Effects of mucosal sodium removal on cell volume in *Necturus* gallbladder epithelium. *American Journal of Physiology.* 249:C304–C312.

Diamond, J. M. 1962. The mechanism of water transport by the gall-bladder. *Journal of Physiology.* 161:503–527.

Diamond, J. M. 1964. The mechanism of isotonic water transport. *Journal of General Physiology.* 48:15–42.

Diamond, J. M. 1978. Solute-linked water transport in epithelia. *In* Membrane Transport Processes. Vol. 1. J. F. Hoffman, editor. Raven Press, New York. 257–276.

Diamond, J. M. 1979. Osmotic water flow in leaky epithelia. *Journal of Membrane Biology.* 51:195–216.

Diamond, J. M., and W. H. Bossert. 1967. Standing-gradient osmotic flow. A mechanism for coupling of water and solute transport in epithelia. *Journal of General Physiology.* 50:2061–2083.

Fisher, R. S., B.-E. Persson, and K. R. Spring. 1981. Epithelial cell volume regulation: bicarbonate dependence. *Science.* 214:1357–1359.

Hill, A. 1980. Salt-water coupling in leaky epithelia. *Journal of Membrane Biology.* 56:177–182.

Hill, A. E. 1975a. Solute-solvent coupling in epithelia: a critical examination of the standing-gradient osmotic flow theory. *Proceedings of the Royal Society of London, Series B.* 190:99–114.

Hill, A. E. 1975b. Solute-solvent coupling in epithelia: an electro-osmotic theory of fluid transfer. *Proceedings of the Royal Society of London, Series B.* 190:115–134.

Hill, A. E., and B. S. Hill. 1978. Sucrose fluxes and junctional water flow across *Necturus* gallbladder epithelium. *Proceedings of the Royal Society of London, Series B.* 200:163–174.

Holz, R., and A. Finkelstein. 1970. The water and nonelectrolyte permeability induced in thin lipid membranes by the polyene antibiotics nystatin and amphotericin B. *Journal of General Physiology.* 56:125–145.

House, C. R. 1974. Water Transport in Cells and Tissues. Edward Arnold Ltd., London. 562 pp.

Ikonomov, O., M. Simon, and E. Frömter. 1985. Electrophysiological studies on lateral intercellular spaces of *Necturus* gallbladder epithelium. *Pflügers Archiv.* 403:301–307.

Marban, E., T. J. Rink, R. W. Tsien, and R. Y. Tsien. 1980. Free calcium in heart muscle at rest and during contraction measured with Ca^{2+}-sensitive microelectrodes. *Nature.* 286:845–850.

Neher, E., and H. D. Lux. 1973. Rapid changes of potassium concentration at the outer surface of exposed single neurons during membrane current flow. *Journal of General Physiology.* 61:385–399.

Pedley, T. J., and J. Fischbarg. 1980. Unstirred layer effects in osmotic water flow across gallbladder epithelium. *Journal of Membrane Biology.* 54:89–102

Persson, B.-E., and K. R. Spring. 1982. Gallbladder epithelial cell hydraulic water permeability and volume regulation. *Journal of General Physiology.* 79:481–505.

Reuss, L. 1983. Basolateral KCl co-transport in a NaCl-absorbing epithelium. *Nature.* 305:723–726.

Reuss, L. 1984. Independence of apical membrane Na^+ and Cl^- entry in *Necturus* gallbladder epithelium. *Journal of General Physiology.* 84:423–445.

Reuss, L. 1985. Changes in cell volume measured with an electrophysiologic technique. *Proceedings of the National Academy of Sciences.* 82:6014–6018.

Reuss, L. 1989. Ion transport across gallbladder epithelium. *Physiological Reviews.* In press.

Reuss, L., and J. L. Costantin. 1984. Cl^-/HCO_3^- exchange at the apical membrane of *Necturus* gallbladder. *Journal of General Physiology.* 83:801–818.

Reuss, L., and C. U. Cotton. 1988. Isosmotic fluid transport across epithelia. *In* Contemporary Nephrology. Vol. 4. S. Klahr and S. G. Massry, editors. Plenum Publishing Co., New York. 1–37.

Reuss, L., and A. L. Finn. 1977. Effects of luminal hyperosmolality on electrical pathways of *Necturus* gallbladder. *Americal Journal of Physiology.* 232:C99–C109.

Reuss, L., and J. S. Stoddard. 1987. Role of H^+ and HCO_3^- in salt transport in gallbladder epithelium. *Annual Review of Physiology.* 49:35–49.

Sackin, H., and E. L. Boulpaep. 1975. Models for coupling of salt and water transport. *Journal of General Physiology.* 66:671–733.

Schafer, J. A., C. S. Patlak, and T. E. Andreoli. 1975. A component of fluid absorption linked to passive ion flows in the superficial pars recta. *Journal of General Physiology.* 66:445–471.

Schafer, J. A., C. S. Patlak, and T. E. Andreoli. 1977. Fluid absorption and active and passive ion flows in the rabbit superficial pars recta. *American Journal of Physiology.* 233:F154–F167.

Schafer, J. A., C. S. Patlak, S. L. Troutman, and T. E. Andreoli. 1978. Volume absorption in the pars recta. II. Hydraulic conductivity coefficient. *American Journal of Physiology.* 234:F340–F348.

Smulders, A. P., J. McD. Tormey, and E. M. Wright. 1972. The effect of osmotically induced water flows on the permeability and ultrastructure of the rabbit gallbladder. *Journal of Membrane Biology.* 7:164–197.

Spring, K. R. 1983. Fluid transport by gallbladder epithelium. *Journal of Experimental Biology.* 106:181–194.

Weinman, S. A., and L. Reuss. 1984. Na^+-H^+ exchange and Na^+ entry across the apical membrane of *Necturus* gallbladder. *Journal of General Physiology.* 83:57–74.

Weinstein, A. M., and J. L. Stephenson. 1981. Models of coupled salt and water transport across leaky epithelia. *Journal of Membrane Biology.* 60:1–20.

Whitlock, R. T., and H. O. Wheeler. 1964. Coupled transport of solute and water across rabbit gallbladder epithelium. *Journal of Clinical Investigation.* 43:2249–2265.

Wright, E. M., A. P. Smulders, and J. McD. Tormey. 1972. The role of the lateral intercellular spaces and solute polarization effects in the passive flow of water across the rabbit gallbladder. *Journal of Membrane Biology.* 7:198–219.

Zeuthen, T. 1982. Relations between intracellular ion activities and extracellular osmolarity in *Necturus* gallbladder epithelium. *Journal of Membrane Biology.* 66:109–121.